Raman spectroscopy of coated pharmaceutical tablets and physical models for multivariate calibration to tablet coating thickness

John F. Kauffman [a],[*], Marybeth Dellibovi [a], Charles R. Cunningham [b]

[a] *FDA, Center for Drug Evaluation and Research, Division of Pharmaceutical Analysis,*
1114 Market St., St. Louis, MO 63101, United States
[b] *Colorcon, Pharmaceutical Technical Services, 415 Moyer Blvd., West Point, PA 19486, United States*

Abstract

Raman spectra of a set of coated pharmaceutical tablets were analyzed for the purpose of calibrating the spectra to tablet coating thickness. Acetaminophen tablets were coated with a hydroxypropylmethylcellulose/polyethylene glycol film coating whose thickness was varied from 0 to 6% weight gain. Coatings were also prepared with two concentrations of TiO_2 at several film thicknesses. The resulting spectral data set was analyzed using several different multivariate calibration procedures. The procedures examined in this study included spectral correction followed by target factor analysis, spectral correction with baseline subtraction followed by principal component regression, and first derivative computation followed by principal component regression. The results demonstrate that target factor analysis is a viable method for calibration of Raman spectra to tablet coating thickness. Calibration based on derivative spectra resulted in linear correlation that was equal to that of the results of target factor analysis for coatings without TiO_2. However, target factor analysis was found to be superior to other methods when TiO_2 was present in the tablet coatings. The effect of sample fluorescence on each of these chemometric methods was also examined. It was found that when photobleaching of fluorescent impurities due to exposure to the Raman excitation source was controlled, the tablet coating thickness could be calibrated to the intensity of the fluorescence signal. The results also demonstrate that for the samples examined here, calibration by target factor analysis is insensitive to variation in fluorescent intensity when the tablet coating emission spectrum is included in the matrix of target vectors.
© 2006 Elsevier B.V. All rights reserved.

Keywords: Tablet coating analysis; Raman spectroscopy; Multivariate calibration; Chemometrics; Target factor analysis

1. Introduction

Many pharmaceutical tablets are coated. Most coatings play a passive role in the behavior of the drug product, serving as protective layers, cosmetic and product branding devices, and aids to ingestion. However, active and functional coatings are becoming more commonplace. For example, enteric coatings determine the location of drug release, and many controlled release products deliver an immediate dose via a quickly dissolving coating over a delayed release core. Furthermore common coating operations are inherently variable, relying on the statistical likelihood that each tablet will be exposed to the same distribution of the coating formulation to produce a uniformly coated tablet batch. Finally, the coating process occurs near the end of the value chain, and

therefore variability or operational errors at this stage in the manufacturing process can have a relatively large financial penalty.

Despite these drivers, relatively little work has been published on the application of non-destructive methods of analysis to coated pharmaceutical tablets. Kirsch and Drennen [1,2] showed that near infrared (NIR) spectra can be calibrated to tablet coating thickness of ethylcellulose and hydroxypropylmethylcellulose film coatings using partial least squares regression (PLS). They also calibrated the ethylcellulose spectra to dissolution time and coated tablet hardness. Han and Faulkner [3] used univariate analysis at a single wavelength to show that NIR spectra are highly correlated with tablet weight gain due to coating. They noted that the coating attenuates the signal from the active pharmaceutical ingredient (API) in the tablet core, and discussed the implication of this effect for measurement of API content uniformity between tablets. Andersson et al. [4] demonstrated the use of NIR spectroscopy to measure tablet coating thickness on combination tablets composed of two parts with different

---

* Corresponding author. Tel.: +1 314 539 2168; fax: +1 314 539 2113.
E-mail address: John.Kauffman@fda.hhs.gov (J.F. Kauffman).

compositions. Using principal component analysis (PCA) they showed that the two sides of the tablet were distinguishable, and PLS was used to develop a quantitative calibration of the spectra to tablet coating thickness for each side of the tablet. Andersson et al. [5] also demonstrated the use of in-line NIR spectrometry to monitor pellet coating in a fluid bed coater. Romero-Torres et al. [6] recently correlated Raman spectra of coated tablets with residence time in a pan coater using PLS. They evaluated the influence of data transformation prior to PLS analysis on the prediction variance of the PLS models. Raman spectroscopy was shown to be a useful method for analysis of tablet-to-tablet variation of coating thickness.

Empirical models based on abstract factors (e.g., PLS models) are extremely useful for finding correlations between response and predictor variables, particularly when the relationship between variables is confounded. However, mechanistic or physical models can often be invoked to explain correlations between spectroscopic variables and response variables, leading to simpler, more efficient calibration methods. Cogdill and Anderson [7] presented the Net Analyte Signal (NAS) and Wiener filters as particularly useful methods for efficient calibration. Both filters begin by dividing the calibration matrix into the sum of an analyte signal vector and a "noise" matrix that includes contributions from all of the interfering spectral components. The NAS method takes the additional step of projecting the analyte pure component spectrum onto a space that is orthogonal to the noise matrix. These methods provide the analyst with tools for the efficient identification of the regression vector that transforms a matrix of calibration spectra to the concentration vector of the analyte of interest. Nadler and Coifman have shown that, for noise free spectra, the regression vector for the analyte of interest identified by PLS is the scaled NAS. [8] Thus in certain cases, computation of the NAS regression vector can provide an adequate, efficient calibration without the extensive data sets that are often required for PLS. Marbach [9,10] noted that, in the limit of noise-free spectra, the Wiener filter identifies the scaled pure component spectrum of the analyte of interest as the optimum regression vector. These results imply that classical least squares (CLS) regression may be an ideal calibration method for noise-free spectra, as long as the measured spectra are additive in the pure components.

Textbook CLS utilizes the measured spectra of the calibration samples and the known concentrations of the pure components to give a least squares estimate of the pure component spectral matrix, which is then inverted to provide a regression vector that calibrates measured spectra to pure component concentrations. Though CLS is one of the simplest calibration methods, it is seldom evaluated during a typical chemometric method development regimen. This may be a consequence of the historical development of chemometrics, the desire to avoid assumptions about the linear additivity of the component spectra (though this assumption is also invoked in the NAS and Wiener filter methods), or a lack of complete knowledge of the pure component spectra. In pharmaceutical sciences, the latter issue is often inconsequential, because the raw material spectra can typically be measured independently. Target factor analysis (TFA) can be used to determine the best linear unbiased estimator of the rota-

tion matrix that projects a pure component vector (target factor) onto the spectral vector space defined by the calibration matrix loadings. Thus, TFA provides a straightforward procedure for performing CLS in reverse. That is, the measured spectra of the calibration samples and the known spectra of the pure components can be used to determine a least squares estimate of the pure component concentrations. These can then be tested against the known pure component concentrations to evaluate the validity of the assumptions underlying the CLS method. Utilizing the pure component spectra to predict concentrations maximizes the use of a priori information, since the number of signal channels in modern spectroscopic instrumentation often exceeds the number of spectra in a typical calibration matrix. TFA has the added advantage that it offers a method to validate the hypotheses from which physical models are derived (e.g., linear additivity of pure component spectra), and this can lead to simple strategies for process control utilizing spectroscopic information. Thus, TFA has all of the characteristics of an efficient calibration method.

The purpose of this paper is to develop TFA for calibration of Raman spectra to tablet coating thickness based on physical models of the spectral composition. The physical model utilized in this research is quite simple. (1) It is postulated that the coating's contribution to the analytical signal increases linearly with coating thickness. (2) It is postulated that the contribution to the analytical signal from the tablet core decreases linearly with increasing coating thickness. (3) It is assumed that the total analytical signal is a linear combination of the coating and core signals. Physically meaningful target vectors (physical factors) were derived from these postulates and the spectral data, and multivariate statistical methods were applied to validate the hypothesis by deriving calibration plots from the scores upon the physical factors. Calibrations based on both an increase in the coating signal and a decrease in the core signal can be developed using this approach. This model was applied to Raman spectra of tablets coated with a hydroxypropylmethylcellulose film with polyethylene glycol as plasticizer (HPMC/PEG), with and without TiO_2 colorant. The influence of computational preprocessing as well as physical preprocessing (sample photobleaching) on the calibration of Raman spectra to tablet coating thickness were also examined. TFA takes advantage of the fact that the analyst has access to independently measured coating and core spectra, information that is not utilized explicitly by PLS models. The calibration model examined in this paper derives from physical spectra rather than abstract spectra, and as a result such a model can be adapted to variations in raw material spectral properties in a straightforward manner.

2. Experimental

2.1. Sample preparation

Tablets containing acetaminophen (APAP, 81%), partially pregelatinized starch, microcrystalline cellulose, polyvinyl pyrrolidone, and stearic acid were prepared using a direct blend technique. The blend was compressed using a compaction force of approximately 12 kN, and the resulting tablet breaking force was 14.9 ± 0.6 kilopounds (klb). The target tablet mass was

Table 1
Target and average measured masses of coated tablets

Tablet number	Target coating thickness (% weight gain)	Average tablet mass (g)	Mass standard deviation (%)	Measured coating thickness[a] (% weight gain)
Uncoated	0.00	0.3973	0.87	0.00
FS1-N-0.5	0.50	0.4007	0.84	0.86
FS1-N-1	1.00	0.4043	0.71	1.76
FS1-N-2	2.00	0.4077	1.33	2.62
FS1-N-3	3.00	0.4096	0.74	3.10
FS1-N-6	6.00	0.4207	1.02	5.89
FS1-L-1	1.00	0.4024	1.04	1.28
FS1-L-3	3.00	0.4104	1.37	3.30
FS1-H-1	1.00	0.3999	0.87	0.65
FS1-H-3	3.00	0.4081	1.03	2.72

[a] Measured coating thickness was calculated as the difference between the average measured coated tablet mass and the average measured uncoated tablet mass.

400 mg, and the measured tablet mass was 397 ± 3 mg. A set of systematically varied coatings were applied to the tablets using an O'Hara model Labcoat II-X, equipped with a 15 in. diameter, fully perforated, side vented pan. The coating is denoted Film System #1 (FS1), and is composed of hydroxypropyl methylcellulose (HPMC), polyethylene glycol (PEG), and TiO_2 as colorant. (A second coating denoted Film System #2 has also been examined, and will be the subject of a separate paper.) Colorant is present in two concentrations: 12% (low concentration, denoted as -L- in the sample numbering scheme) and 31.25% (high concentration, denoted as -H-). Coatings without TiO_2 are denoted as -N- in the sample numbering scheme. Coatings of several thicknesses were prepared by varying the residence time in the tablet coater. The coating thickness, characterized as the target percent weight gain of the tablet, is denoted by the last number in the coating sample number. The sample numbers and descriptions for the FS1 set of coated tablets and their measured average percent weight gains versus the average measured mass of the uncoated tablets are given in Table 1.

2.2. Measurement and data analysis

Raman spectra were measured with a ChemImage Corp. (Pittsburgh, PA) Falcon II Molecular Chemical Imaging System. The instrument is constructed around an Olympus BX51 microscope, and utilizes a Coherent Verdi 532 nm laser excitation source. Integrated closed-loop feedback systems control the laser frequency, temperature and output power, resulting in output stability of $\pm 1\%$ of the power set point. A video camera is available for brightfield transmission or reflectance imaging with white light illumination. In the studies described here, brightfield reflectance imaging was used for initial focusing of the microscope onto the surface of the tablets. For Raman spectral measurements, the 532 nm excitation is directed through the microscope objective and onto the sample, and backscattered Raman radiation is collected by the same objective. The Rayleigh scattering is removed from the collected radiation with a dielectric longpass filter, and the Raman scattered light is directed through a triple-grating 0.5 m monochromator onto a CCD camera for measurement of the Raman spectrum of the illuminated field of view of the microscope. Spectra for this

study were recorded using a 300 groove/mm grating, to give spectral resolution of $13 \, cm^{-1}$, and a spectral range in excess of $4000 \, cm^{-1}$. The instrument's spectral response function was determined using a NIST SRM 2422 Raman intensity standard. All spectra measured in this work were collected through 5× or 20× objectives as noted in the text. The laser illumination has a Gaussian beam diameter of approximately 485 µm at the surface of the sample when the 5× objective is used, and 110 µm when the 20× objective is used.

Each spectrum for coating thickness calibration was measured with a 5× objective using 10 s of total exposure time during the measurement and 200 mW of excitation power as measured at the source. The laser throughput of the optical system with the 5× objective is 42%, and therefore the power density at the sample was $45 \, W/cm^2$. The sampled region of each tablet was irradiated with the excitation source for 360 s immediately prior to measurement of its Raman spectrum in order to photobleach fluorescent impurities in a controlled fashion. Each spectrum for the photobleaching study was measured with a 20× objective using 10 s of total exposure time during the measurement, and 120 mW of excitation power. The laser throughput of the optical system with the 20× objective is 28%, and therefore the power density during photobleaching was $355 \, W/cm^2$. Multivariate statistical analysis of the spectral data was performed using in-house software implemented in Microsoft Excel using Visual Basic for Applications. Principal component analysis was performed using the singular value decomposition method. The Visual Basic program written to implement his method utilized the XNumbers Multiprecision Floating Point Add-in [11] and the Matrix Functions and Linear Algebra Add-in [12]. Both of these open source freeware utilities are available online. Principal component analysis in Excel was validated by comparison with analysis of the same data sets using the commercially available Pirouette (Infometrix, Bothell, WA) software package.

3. Target factor analysis

Target factor analysis can be utilized to validate the hypothesis that the analytical signal is a linear combination of the core spectrum and the coating spectrum. Any $M \times N$ dimensional

data matrix, $\mathbf{D}$, can be factored into its principal components [13,14]

$$\mathbf{D} = \mathbf{UT} \tag{1}$$

where $\mathbf{U}$, the loadings matrix, is an $M \times N$ dimensional orthonormal matrix of principal components that span the spectral space of $\mathbf{D}$, and $\mathbf{T}$, the scores matrix, is an $N \times N$ dimensional orthogonal matrix. ($\mathbf{T}$ is the product of the diagonal singular value matrix and the matrix of right singular vectors that form an orthonormal basis for the vector space defined by the columns of $\mathbf{D}$.) M is the number of channels in the spectrum and N is the number of spectra in the calibration matrix. The formalism developed here assumes that the spectra, d_i, that comprise $\mathbf{D}$ are arranged in columns. The K-rank data matrix, $\mathbf{D}_K$, can be reconstructed from the $\mathbf{U}$ and $\mathbf{T}$ by matrix multiplication of the first K principal components (columns of $\mathbf{U}$) and the first K scores vectors (rows of $\mathbf{T}$) in Eq. (1). When rank reduction is performed properly, the retained principal components span the physical space of $\mathbf{D}$, and ideally only random variance (i.e., noise) has been eliminated. The principal components can be transformed into physically meaningful basis vectors for $\mathbf{D}$ by a non-orthogonal rotation, [15].

$$\mathbf{D}_K = \mathbf{U}_K \mathbf{R}_K \mathbf{R}_K^{-1} \mathbf{T}_K = \mathbf{AC} \tag{2}$$

where $\mathbf{R}$ is a square rotation matrix of rank K, $\mathbf{A}$ is the matrix of K physically meaningful spectra (physical factors), and $\mathbf{C}$ is a matrix of physical scores upon the spectra in $\mathbf{A}$. The row vectors of $\mathbf{C}$ are often proportional to the concentrations of the species whose spectra comprise the $\mathbf{A}$ matrix. The relationship between $\mathbf{C}$ and the concentration measure of interest (in this paper, tablet coating thickness) can be used for multivariate calibration.

From Eq. (2), it is apparent that

$$\mathbf{U}_K \mathbf{R}_K = \mathbf{A} \tag{3}$$

and

$$\mathbf{R}_K^{-1} \mathbf{T}_K = \mathbf{C} \tag{4}$$

Target factor analysis (TFA) can be used to validate the rotation matrix required in Eq. (2) by hypothesizing that a set of target vectors, $\mathbf{P}$, is an adequate representation of $\mathbf{A}$. Substituting $\mathbf{P}$ for $\mathbf{A}$ in Eq. (3), the best linear unbiased estimator of the rotation matrix can be calculate as:

$$\mathbf{R}_{K,\text{test}} = \mathbf{U}_K^T \mathbf{P} \tag{5}$$

Eq. (5) makes use of the orthonormality of the $\mathbf{U}$ matrix. The hypothesis is then tested by computing the test vectors,

$$\mathbf{A}_{\text{test}} = \mathbf{U}_K \mathbf{R}_{K,\text{test}} \tag{6}$$

and comparing $\mathbf{A}_{\text{test}}$ to $\mathbf{P}$. Eqs. (5) and (6) demonstrate that the test vectors are projections of the target vectors onto the vector space defined by $\mathbf{U}$, and the idempotent property of the projection matrix, $\mathbf{M}_K = \mathbf{U}_K \mathbf{U}_K^T$, assures the redundancy of repeating the procedure. Thus, $\mathbf{A}_{\text{test}}$ is the best least squares estimate of the projection of $\mathbf{P}$ onto $\mathbf{U}$. The rotation matrix calculated by Eq. (5) can be used to find $\mathbf{C}$ via Eq. (4), and the relationship between $\mathbf{C}$ and the concentration measure of interest can also be

tested for linearity. When the hypothesis is found to be true, TFA can lead to simple calibration schemes, because the calibration procedure is reduced to linear regression of $\mathbf{D}$ onto $\mathbf{A}_{\text{test}}$. When this approach is applied to process control, it also provides a clear procedure for modifying the method when adjustments for changes in raw material spectral properties are required.

The variance between $\mathbf{A}_{\text{test}}$ and $\mathbf{P}$, S^2_{total}, is the sum of two independent contributions; S^2_{data}, the variance contained in the N-K insignificant loadings (i.e., random noise), and S^2_{TFA}, the variance assigned to differences between the target vectors of $\mathbf{P}$ and the test vectors of $\mathbf{A}_{\text{test}}$. Lorber [15] has used the projection matrix formalism to derive expressions for S^2_{total} and S^2_{data}, and he has used geometric arguments to derive an expression for S^2_{TFA}. S^2_{TFA} and S^2_{data} can be used in a one-sided F-test to test the null hypothesis that S^2_{TFA} is insignificant compared to S^2_{data}. If the ratio

$$F_{\text{geometric}} = \frac{S^2_{\text{TFA}}}{S^2_{\text{data}}} \tag{7}$$

is less than the F-value for a specified confidence level, then the null hypothesis is accepted, and the target vector is considered a valid component of the physical factor matrix, $\mathbf{A}$. When the use of S^2_{TFA} and S^2_{data} result in an F-value that is negative or undetermined, Lorber recommends an alternative form based on independent error measures, F_{alt} (see Eq. (29) in ref. [11]). Thus, rigorous statistical tests can be applied to test the hypothesis $\mathbf{A} = \mathbf{P}$.

4. Calibration based on coating fluorescence and core Raman

Fig. 1 shows a series of raw, unprocessed spectra of a single FS1-N-2 tablet measured following varying exposure times of the sampled region to the excitation laser. The Raman features in the 0 min spectrum appear attenuated because the signal has exceeded the 16 bit dynamic range of the CCD camera, but the 3, 6 and 9 min spectra have nearly identical Raman intensities superimposed on a temporally decreasing fluorescent
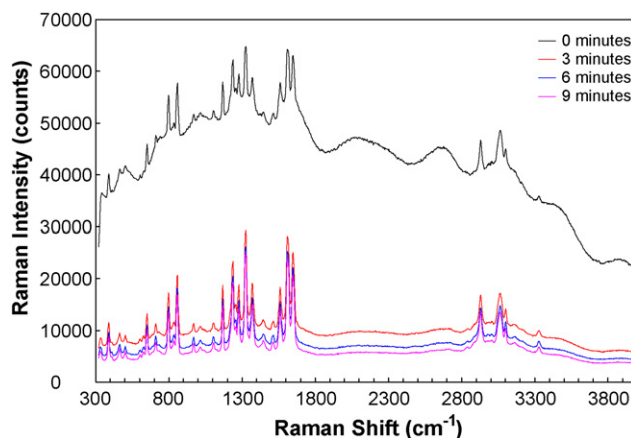

Fig. 1. Raman spectra of a single FS1-N-2 tablet after varying laser exposure times. The broad oscillations observed in the spectra reflect the instrument optical transmission function.
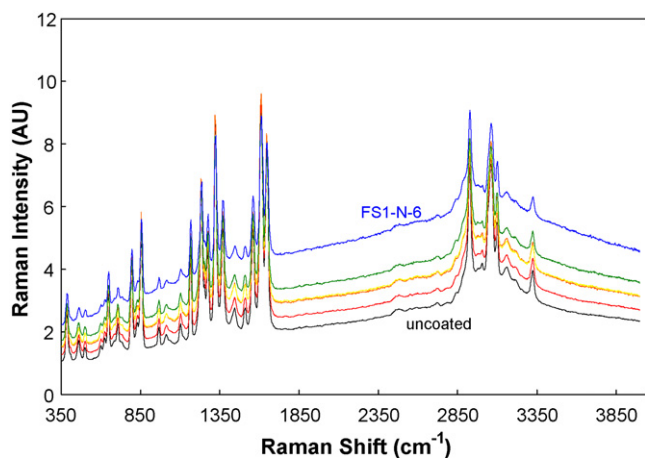
Fig. 2. Average Raman spectra of the FS1-N-X series of spectra consisting of acetaminophen tablets coated with a HPMC/PEG film coating. The coating does not contain TiO_2, and only the coating thickness has been varied between spectra. The order of the spectra from lowest to highest baseline is uncoated, FS1-N-0.5, FS1-N-1, FS1-N-2, FS1-N-3 and, FS1-N-6.

background. This is characteristic of photobleaching of fluorescent impurities in the sample matrix, which are present in both the tablet core and the coating. Though the background fluorescence is present in both core and coating, photobleaching studies of coated tablet cross-sections reveal that the coating fluorescence is more persistent than that of the core. Extensive study of photobleaching in a broad variety of coated tablets revealed a systematic variation in the magnitude of the fluorescence signal with increasing coating thickness when the laser exposure time was fixed to control the extent of photobleaching. All data displayed in the remainder of this article were collected following 6 min of photobleaching, unless noted otherwise.

Fig. 2 displays the FS1-N-X series of spectra, in which only the coating thickness varies between spectra. Each spectrum in the figure is the average of the spectra of 10 randomly selected tablets from its coating thickness category, and each spectrum has been spectrally corrected using the instrument's spectral response function. Division by the spectral response function alters the intensity measure for all spectra equally, but the units become arbitrary (AU). The spectrum of the coating consists primarily of fluorescence, with a broad weak Raman peak in the 2800–3000 cm^{-1} region of the spectrum (see Fig. 3A). All of the strong, sharp features in Fig. 2 can be attributed to acetaminophen peaks from the tablet core. As the coating thickness increases, the baseline is observed to increase, and the intensities of the sharp features are observed to decrease. Principal component decomposition and subsequent analysis of the singular values indicates that two factors are required to model the data.

The hypothesis concerning the composition of the spectra shown in Fig. 2 was evaluated by preparing a test matrix consisting of the uncoated tablet spectrum and the measured spectrum of a tablet coating that was sliced from a FS1-N-6 tablet. Fig. 3A displays the normalized target vectors that comprise **P** along with the predicted spectra that comprise **A**. The predicted tablet core spectrum is nearly identical to the target factor, which is expected since the target factor is also a vector in the data
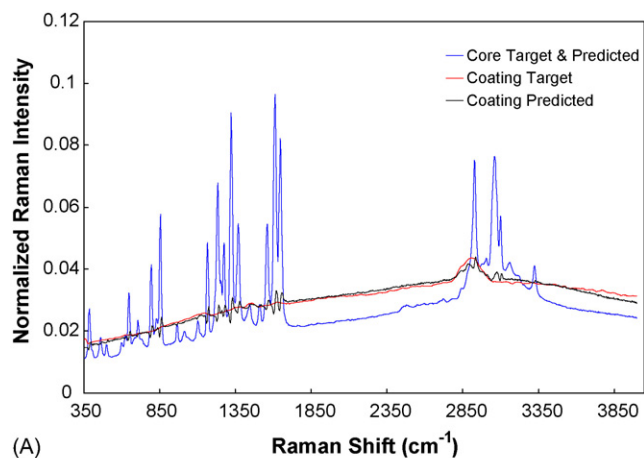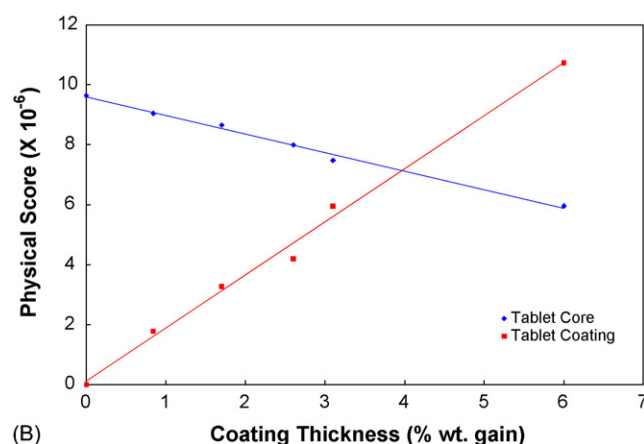
Fig. 3. (A) Target factors and predicted vectors for the data shown in Fig. 2. The tablet core predicted vector is identical to the target vector, and is therefore not apparent as a separate spectrum. The predicted coating vector is identical to a difference spectrum calculated from the data matrix. (B) Scores on the physical factors shown in A. The lines show linear regression fits of the scores to coating thickness. The coating thicknesses are values measured as average weight gain for a representative sample of 10 tablets.

matrix. The predicted spectrum of the tablet coating resembles a spectrum constructed as the difference between a coated tablet spectrum and an uncoated tablet spectrum whose amplitude has been scaled to adjust for attenuation of the tablet core's contribution. The tablet coating target vector has the appearance of a highly smoothed difference spectrum. The main difference between target and predicted vectors is the presence of oscillations in the vicinity of the strong Raman peaks of the tablet core spectrum. The first derivative appearance of the noise peaks suggests that they arise from small variations on the rising and falling edges of the sharp Raman bands. When the tablet coating target factor is constructed as a difference spectrum based on the spectra in **D**, the target and predicted vectors are identical, and the predicted vector is also identical to the predicted vector shown in Fig. 3A.

The statistical test described in Section 3 has been applied to each pair of target and predicted vectors shown in Fig. 3A. The *F*-ratio for the tablet core target spectrum was computed using the method proposed by Lorber [15] (see Eq. (29) in ref. [11]), and results in a value of nearly zero. This is to be expected, because

the target factor associated with the tablet core spectrum is taken directly from the data matrix, and therefore the component of this target vector orthogonal to the reduced rank data matrix will be nearly zero. The F-ratio for the target vector associated with the tablet coating has a value of 0.05, indicating that S^2_{TFA} is an order of magnitude smaller than S^2_{data}. Thus, the null hypothesis that $\mathbf{P} = \mathbf{A}$ is accepted.

Fig. 3B displays a plot of the physical scores contained in the rows of $\mathbf{C}$ when $\mathbf{D}$ is projected onto $\mathbf{A}$. The physical scores are plotted against the average tablet coating thickness for each thickness category, displayed as the percent weight gain. Inspection of the coatings by brightfield reflectance microscopy indicates that 1% weight gain corresponds to a thickness of 14 μm. The scores upon the uncoated tablet spectrum decrease linearly with increasing coating thickness, indicating that the coating attenuates the core Raman spectrum, as anticipated. The scores upon the coating spectrum indicate that the fluorescence background increases linearly with an increase in coating thickness. The fact that both sets of scores appear to be linearly dependent on tablet coating thickness is consistent with the hypothesis presented in Section 1. Linear regression of the data in Fig. 3B give linear correlation coefficients of 0.99 for both the tablet core and tablet coating scores, and the best fit models for the dependence of the physical scores on coating thickness are $C_{core}(\delta) = -618{,}136\delta + 10^7$ and $C_{coating}(\delta) = 2 \times 10^6\delta + 119{,}146$ for the tablet core and coating scores, respectively, where δ is the coating thickness. These equations can be inverted to give the tablet coating thickness as a function of the scores on the core and coating target factors.

5. Calibration based on attenuation of the core Raman signal

Fig. 3 demonstrates that tablet coating thickness can be calibrated to attenuation of the Raman spectrum of the tablet core as well as the emission spectrum of the coating. Observation of the linear dependence of the tablet coating scores on coating thickness as seen in Fig. 3B requires careful control of photobleaching. However, the successful decomposition of the Raman spectra of coated tablets into the sum of contributions from an attenuated core spectrum and a coating spectrum implies that the projection of $\mathbf{D}$ onto $\mathbf{A}$ can be used to subtract the coat-

ing spectrum from measured spectra of coated tablets. If this is found to be true, then control of photobleaching should not be required to develop a linear calibration using core attenuation only. This hypothesis has been tested by examining the FS1-N-X tablet spectra following varying degrees of photobleaching. Spectra of single tablets were collected after 0, 3, 6 and 9 min photobleaching times to generate data sets for each of the six coating thicknesses. For example, the FS1-N-2 data set is shown in Fig. 1. In most cases the initial spectra (0 min photobleaching) contain so much fluorescence that the detector was saturated at some frequencies, and therefore the initial spectra were not used for further analysis. The remaining 18 spectra were compiled into a single data matrix, and target factor analysis was applied using the target vectors shown in Fig. 3A. The scores upon the target factors are tabulated in Table 2. Within each coating thickness category, the scores on the attenuated core spectrum are nearly identical, even though the background fluorescence level of the spectra vary dramatically. The standard deviations of the measured scores on the core spectra of individual tablets range from 0.1 to 0.4%. A systematic variation with coating thickness is also evident. In contrast, the coating emission scores in Table 2 show large, systematic variations with increasing exposure to the excitation source within coating thickness categories. The results in Table 2 demonstrate that TFA provides adequate calibration of coating thickness to attenuation of the Raman core signal even when photobleaching of impurity fluorescence is not carefully controlled. In effect, TFA is capable of subtracting the coating emission spectrum from the data vector without influencing the information contained in the core Raman spectrum.

In view of these results, the reliability of a single factor model following subtraction of the baseline from the spectra shown in Fig. 2 has been examined. The baseline of each spectrum shown in Fig. 2 was fit to a third order polynomial, and the resulting baseline model was subtracted from the spectrum to generate the baseline corrected spectrum. Principal component analysis indicated that the resulting data could be adequately described with a single factor model. Scores on the first principal component (PC) following baseline subtraction are plotted against coating thickness in Fig. 4.

The scores exhibit a linear dependence on coating thickness with a negative slope, indicating that the scores on the first PC

Table 2
Scores on target factors for spectra with varying photobleaching times

| | Scores on core spectrum[a] ($\times 10^{-6}$) | | | | | | Scores on coating spectrum[a] ($\times 10^{-6}$) | | | | | |
	0[b]	0.84[b]	1.7[b]	2.6[b]	3.1[b]	5.9[b]	0[b]	0.84[b]	1.7[b]	2.6[b]	3.1[b]	5.9[b]
3 min	9.08	7.77	7.57	6.55	4.90	4.22	−1.32	1.76	1.49	4.97	7.35	8.86
6 min	9.10	7.79	7.58	6.56	4.91	4.24	−2.63	−0.32	−0.49	2.30	4.03	5.32
9 min	9.13	7.81	7.59	6.59	4.91	4.25	−3.27	−1.27	−1.39	0.99	2.45	3.73
Average	9.10	7.79	7.58	6.57	4.91	4.24	−2.40	0.06	−0.13	2.75	4.61	5.97
R.S.D.[c] (%)	0.3	0.2	0.2	0.3	0.1	0.4	−41	2668	−1152	74	54	44

[a] Spectra from single tablets within each coating category were compiled into the data set, followed by principal component decomposition and target factor analysis.

[b] Nominal coating thickness (% wt. gain).

[c] Relative standard deviations are given as a percent of the average value of the score within each coating thickness category.
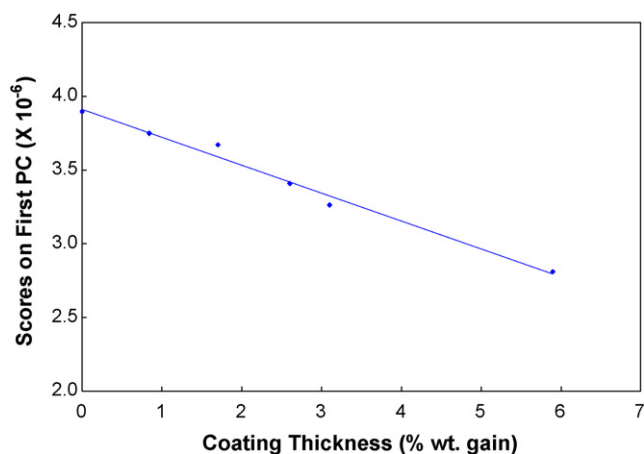
Fig. 4. Scores on the first principal component of the data shown in Fig. 2 following baseline subtraction.

from the baseline subtracted spectra reflect attenuation of the tablet core contribution to the spectrum. The linear correlation coefficient of the plot shown in Fig. 4 is 0.99.

6. Calibration of derivative spectra

Spectral differentiation offers a model-free alternative to subtraction of unwanted background from Raman spectra. Calibration of the spectra shown in Fig. 2 to tablet coating thickness following transformation of the spectra to their first and second derivatives has been examined. All derivative computations were executed by the Savitsky-Golay convolution using a fifth order polynomial and a width of 7 data points. Principal component decomposition of the spectra was performed following derivative computation, and calibration equations were determined by linear regression of the scores on the first principal component against the tablet coating thickness. Projection onto target factors was not necessary in this case, because the first principal component modeled the derivative spectrum of the tablet core Raman spectrum. The calibration equations thus determined were $C_{\text{first derivative}}(\delta) = 2435\delta - 36{,}133$ and $C_{\text{second derivative}}(\delta) = -1698\delta + 24{,}296$ for the first and second derivative scores, respectively. The linear correlation coefficient of each plot was 0.99. These results demonstrate that the scores on the first PC of the data set are correlated with the tablet coating thickness after spectral differentiation. Similar results can be extracted from the data following baseline elimination by other methods, and therefore it is concluded that the correlation between scores on derivative spectra and tablet coating thickness are related to attenuation of the core Raman signal due to the presence of the tablet coating. Thus, spectral differentiation does not distort the information contained in the original spectral data. The results also demonstrate that there is no particular advantage to second derivative computation. The first derivative spectrum provides the same advantage with respect to elimination of the baseline signal.

7. Raman spectra of tablet coatings containing TiO₂

The conclusions drawn from the analysis presented in Sections 4–6 are restricted to coatings that do not contain strongly Raman scattering components. In this section calibration of tablet coating thickness to Raman spectra of coatings containing TiO_2 is considered. Anatase TiO_2 is commonly used as an opaque whitener in tablet coatings. It has four strong Raman bands at approximately 145, 397, 515, and $640 \, \text{cm}^{-1}$. TiO_2 in coatings will affect calibrations described above in two ways. First, it will increase the degree of attenuation of the tablet core Raman signal for a given coating thickness due to the particulate nature of the TiO_2 in the coatings. Secondly, the sharp TiO_2 Raman features in the coating prevent the elimination of the coating emission spectrum by baseline subtraction, and may influence the usefulness of spectral differentiation as a means of eliminating coating emission as well. On the other hand, the TiO_2 spectrum offers the potential for an independent measure of the tablet coating thickness that may be more reliable than coating fluorescence. Thus, a thorough analysis of calibration of tablet coating thickness to Raman spectra of TiO_2-containing coatings is warranted. Calibration has been performed on a set of averaged spectra consisting of the uncoated tablet, the complete FS1-N-X data set shown in Fig. 2, and a set of averaged spectra from the FS1-L-1, FS1-L-3, FS1-H-1, and FS1-H-3 coating categories. Spectra of tablets with coatings containing TiO_2 are shown in Fig. 5. Strong peaks at 397, 515 and $640 \, \text{cm}^{-1}$ increase as the total TiO_2 mass in the coating increases. The FS1-H-3 sample shows the strongest TiO_2 peak intensities, but the lowest fluorescence background. Evidently, the fluorescent background in these samples is no longer strictly correlated with coating thickness. As the TiO_2 concentration in the coating increases, the fluorescence background decreases, in contrast to the effect of increasing coating thickness. The decrease in fluorescence background is the result of dilution of the polymeric compo-
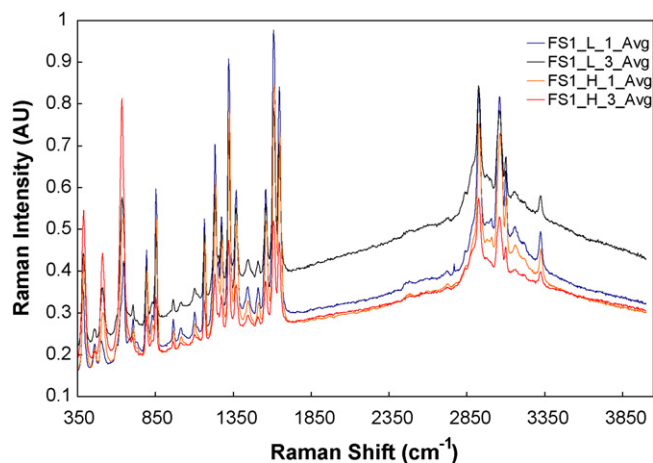

Fig. 5. Average Raman spectra of the FS1-L-X and FS1-H-X series of spectra consisting of acetaminophen tablets coated with a HPMC/PEG/TiO₂ film coating. The FS1-L-X spectra contain TiO₂ at 12% of total solids in the coating, and the FS1-H-X spectra contain TiO₂ at 31.25% of total solids in the coating. Attenuation of the tablet core Raman spectrum is evident in the peak at $\sim 3330 \, \text{cm}^{-1}$.

nents of the coating by the TiO_2 as well as attenuation of the polymer's contribution to the coating signal due to scattering by the TiO_2. The influence of TiO_2 on attenuation of the tablet core Raman spectrum is also evident in Fig. 5. As the concentration of TiO_2 increases, the attenuation of the tablet core Raman signal increases dramatically.

Variation in the concentration of TiO_2 in the tablet coatings influences the intensity of the TiO_2 peaks, the degree of attenuation of the tablet core Raman spectrum, and the observed level of fluorescent background. A complete model of these spectra is expected to require three factors, and this expectation is corroborated by principal component analysis. TFA was performed using the two target factors shown in Fig. 3B, and the measured spectrum of anatase TiO_2 as the third target factor. Statistical analysis of the TiO_2 target factor revealed an F-ratio of 0.45 using Eq. (7), indicating that the TiO_2 spectrum is a valid component of the **A** matrix for the analysis of coated tablets containing TiO_2.

The scores upon the TiO_2 target factor are expected to be correlated with the mass of TiO_2 in the coatings, which is calculated as the percent weight gain of coating times the fraction of solids in the coating formulation due to TiO_2. In addition, if scattering from TiO_2 is the dominant mechanism for attenuation of the tablet core Raman spectrum in these samples, then the scores upon the tablet core target factor are also expected to be correlated with the mass of TiO_2 in the coating. Fig. 6 shows a plot of the scores upon all three component spectra versus TiO_2 mass in the coatings. The results of linear regression for the scores upon the tablet core target factor and the TiO_2 target factor are also shown in Fig. 6. The linear least squares calibration expression for the dependence of tablet core scores on TiO_2 mass is $C_{core}(M) = -8 \times 10^6 M + 10^7$, where M is the mass of TiO_2 in the coating, and the correlation coefficient of the plot is 0.92. Note that the slope of plot is about a factor of 13 steeper than that of the core attenuation calibration in the absence of TiO_2. After accounting for the increase in slope due to rescaling of the x-axis, the presence of TiO_2 in the tablet coatings
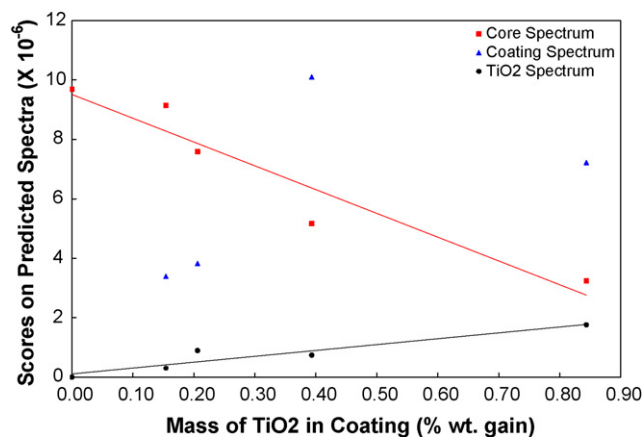

Fig. 6. Scores on physical factors vs. mass of TiO_2 in coating. Linear regression results for scores upon tablet core Raman spectrum and TiO_2 component spectrum are also shown. The mass of TiO_2 in the coating as a percent weight gain is calculated as the coating percent weight gain × fraction of total solids mass due to TiO_2 in the formulation.

appears to result in an increase by a factor of 3.5 of the attenuation of the tablet core Raman spectrum by the coating. The linear least squares calibration equation for the dependence of the TiO_2 scores on TiO_2 mass is $C_{TiO_2}(M) = 2 \times 10^6 M + 114539$, and the correlation coefficient of the plot is 0.90. Thus, it appears that both the increase in the TiO_2 spectrum and the attenuation of the tablet core Raman spectrum can be used to measure tablet coating thickness when the coating contains TiO_2. In contrast, the correlation coefficient of the dependence of the scores upon the coating emission component spectrum on TiO_2 mass is 0.49, indicating poor correlation.

Baseline subtraction prior to TFA of this data set does not improve the model. Without baseline subtraction, three principal components ($K = 3$) were adequate to model the data, but after baseline subtraction four principal components ($K = 4$) were required. These results suggest that when three or more spectral components contribute to the baseline, baseline subtraction removes a linear combination of physical factors rather than predominantly removing a single physical factor as observed in Section 5. In this case TFA will fail, because a three component model will be inadequate to explain the variance in the data, and a four component model requires the inclusion of spectral components that do not have obvious physical significance. When the three component target factor matrix was used in TFA of the baseline subtracted data, the predicted vector associated with the coating emission spectrum was rejected on the basis of analysis of variance described in Eq. (7). Furthermore, correlation coefficients between scores on the predicted vectors and TiO_2 mass were inadequate to provide meaningful calibration of tablet coating thickness. Similar results were obtained when a two factor model was applied to spectra of coatings containing TiO_2 following spectral differentiation. Evidently, it is not possible to establish a meaningful physical model for the Raman spectra of coated tablets following spectral differentiation when the coating contains a strong Raman scatterer of varying intensity. This may result from the fact that the Raman spectrum of APAP has weak peaks that are very close to the peaks in the TiO_2 spectrum, resulting in poor spectral resolution of derivative spectra following TFA. Though baseline subtraction and spectral differentiation generated unsatisfactory results, it is possible that they may still be useful when a single coating formulation is used. Unfortunately, with only two coating thicknesses within each TiO_2 concentration category, it was not possible to test this hypothesis using the existing data sets.

Scores on the target factors are expected to be correlated with the contribution of each spectrum to the overall Raman spectrum of the samples. The scores of the average spectra of tablets without TiO_2 in the coatings (including the uncoated tablet) were analyzed separately by TFA using the three component target factor matrix to determine the influence of a third factor on calibration of the Raman spectra to the tablet coating thickness. The results were very similar to those shown in Fig. 3B. Attenuation of the tablet core Raman spectrum was linearly dependent on tablet coating thickness. Linear regression of the scores against coating thickness resulted in the calibration expression $C_{core}(\delta) = -623{,}678\delta + 10^7$, with a correlation coefficient of 0.99. Scores upon the coating emission spectrum

were also linearly correlated with tablet coating thickness, with a calibration expression $C_{coating}(\delta) = 2 \times 10^6 \delta + 402{,}243$, and a correlation coefficient of 0.96. Scores upon the TiO_2 component spectrum were all less than 1% of the scores on the other factors, indicating that the TiO_2 spectrum is not found in this subset of the data, as expected.

8. Discussion

The studies presented in this paper indicate that TFA is a robust method for resolving Raman spectral components of coated pharmaceutical tablets, as well as the subsequent calibration of the scores upon the Raman spectral components to tablet coating thickness. In some cases other methods such as background subtraction and spectral differentiation have also been shown to be useful for calibration of coated tablet Raman spectra to tablet coating thickness, but TFA appears to be the only method examined in this study that is applicable to all sample sets. In this application, TFA is essentially a sophisticated method for subtraction of unwanted spectral components, and is particularly useful when reasonable models of all spectral components contributing to the data can be estimated. TFA requires minimal data preprocessing, and therefore limits distortion of the raw data due to preprocessing. This feature of TFA is particularly appealing, because the actual spectral components can be utilized for process understanding and process control in product development and manufacturing functions.

One of the key issues in the application of non-destructive spectroscopic testing to pharmaceutical manufacturing is the need to develop calibration models that support information feedback and feedforward for process control. This issue is particularly challenging for batch operations such as tablet coating, because calibration of predictor variables to batch properties nearly always rely to some degree on outcomes of the analysis of prior batches. For instance, application of PLS models to batch process control is complicated by the formal requirement of simultaneous analysis of predictor and response variables. TFA may provide useful models for control of tablet coating processes. The results of this paper demonstrate that TFA can accommodate variations in the spectral properties of the materials delivered to the tablet coating equipment by simply updating the target factors with spectra of the tablets and coating formulation components. For example, if the process control model relies on calibration of the tablet core Raman spectrum attenuation to tablet coating thickness, the operator can simply collect an average spectrum of uncoated tablets prior to the coating operation to account for changes in the tablet core Raman spectrum. Changes in the spectral properties of the coating formulation may also influence the relationship between tablet coating thickness and the degree of attenuation of the tablet core Raman spectrum, but if this relationship depends systematically on the coating formulation Raman spectrum, this effect can also be accommodated using TFA. Similar strategies for utilization of the intensity of the TiO_2 Raman spectrum for control of tablet coating thickness can also be devised.

Photobleaching of impurity fluorescence as a means of pretreating samples prior to analysis of tablet coating thickness raises two important issue related to the practical application of Raman spectroscopy for process control. The first issue is related to the expectation that process analytical technology should be non-destructive. Though the tablets examined in this study remained intact after spectroscopic examination, it is also clear from the observed reduction in background fluorescence that the physical properties of the illuminated region of the tablets were altered by prolonged exposure to the laser excitation source. Photobleaching is a linear effect, and occurs even when tablets are exposed to ambient levels of visible and ultraviolet radiation. Exposure of a small region of the tablet to the laser hastens the photobleaching process in the illuminated region, and appears to reduce the level of fluorescent impurities by a factor of 10 within this region. Fluorescent impurities are expected to be present in sub-part-per-million levels in most samples, so the effect of photobleaching may be insignificant. Nevertheless, until studies are performed to determine the influence of laser illumination on bioavailability and other critical quality attributes, it is best to view photobleaching as a potentially destructive effect.

The second issue concerning photobleaching is related to the time required to illuminate the samples sufficiently to prepare them for measurement. In this study it was deemed essential to control the total exposure of the tablets to the excitation, and the tablets were subjected to 6 min of photobleaching prior to the 10 s spectral measurement. This length of time is impractical for process analytical technology, and therefore it is unlikely that persistent tablet coating fluorescence following prolonged photobleaching will emerge as a viable method for controlling tablet coating operations. However, it was also shown that as long as the maximum signal level did not exceed the dynamic range of the detector, the Raman spectrum of the sample was not distorted by the presence of fluorescent background. This observation essentially eliminates the requirement for photobleaching prior to measurement of the coated tablet Raman spectrum, because the CCD exposure time and integrated collection time can be adjusted to reduce the maximum signal level while maintaining the signal-to-noise level required for accurate calibration based on attenuation of the tablet core Raman spectrum. This strategy has the added benefit of reducing the total exposure time of the tablets, thereby partially mitigating the potentially destructive nature of the measurement.

One additional well-known strategy for minimizing fluorescence is the use of long wavelength laser sources that do not overlap with the absorbance spectra of fluorescent impurities. Identifying a suitable long wavelength source for Raman spectroscopy of coated tablets has three significant advantages. First is obviates the need for photobleaching, and therefore reduces the time required to make a measurement. Secondly, it eliminates concern that the measurement process may alter the sample. Third, it may reduce the coating emission intensity to a level that allows a single variable measurement of tablet coating thickness via attenuation of the tablet core Raman spectrum.

expertise concerning Raman microscopy and Raman chemical imaging.

References

[1] J.D. Kirsch, J.K. Drennen, J. Pharm. Biomed. Anal. 13 (1995) 1273–1281.
[2] J.D. Kirsch, J.K. Drennen, Pharm. Res. 13 (1996) 234–237.
[3] S.M. Han, P.G. Faulkner, J. Pharm. Biomed. Anal. 14 (1996) 1681–1689.
[4] M. Andersson, M. Josefson, F.W. Langkilde, K.G. Wahlund, J. Pharm. Biomed. Anal. 20 (1999) 27–37.
[5] M. Andersson, S. Folestad, J. Gottfries, M.O. Johansson, M. Josefson, K.G. Wahlund, Anal. Chem. 72 (2000) 2099–2108.
[6] S. Romero-Torres, J.D. Perez-Ramos, K.R. Morris, E.R. Grant, J. Pharm. Biomed. Anal. 38 (2005) 270–274.
[7] R.P. Cogdill, C.A. Anderson, J. Near Infrared Spectrosc. 13 (2005) 119–132.
[8] B. Nadler, R.R. Coifman, J. Chemom. 19 (2005) 45–54.
[9] R. Marbach, J. Biomed. Opt. 7 (2002) 130–147.
[10] R. Marbach, J. Near Infrared Spectrosc. 13 (2005) 241–254.
[11] L. Volpi, XNumbers—Multiprecision Floating Point Computation and Numerical Methods for EXCEL [4.5] Foxes Team, 2005.
[12] L. Volpi, MATRIX—Matrix and Linear Algebra for EXCEL [1.9] Foxes Team, 2005.
[13] M.E. Wall, A. Rechtsteiner, L.M. Rocha, A Practical Approach to Microarray Data Analysis, Kluwer Academic Publishers, 2003, pp. 91–109.
[14] E.R. Henry, J. Hofrichter, Numerical Computer Methods, Academic Press, San Diego, 1992, pp. 129–192.
[15] A. Lorber, Anal. Chem. 56 (1984) 1004–1010.